Technische Universität Chemnitz

Sonderforschungsbereich 393

Numerische Simulation auf massiv parallelen Rechnern

Th. Apel V. Mehrmann D. Watkins

Structured eigenvalue methods for the computation of corner singularities in 3D anisotropic elastic structures

Preprint SFB393/01-25

Preprint-Reihe des Chemnitzer SFB 393

SFB393/01-25 **October 2001**

Contents

Thomas Apel
TU Chemnitz
Fakultät für Mathematik
09107 Chemnitz, Germany

na.apel@na-net.ornl.gov
http://www.tu-chemnitz.de/~tap

Volker Mehrmann
TU Berlin
Fakultät für Mathematik
10623 Berlin, Germany

mehrmann@math.tu-berlin.de
http://www.math.tu-berlin.de/~mehrmann

David Watkins
Washington State University
Department of Mathematics
Pullman, WA, 99164-3113, U.S.A.

watkins@math.wsu.edu
http://www.sci.wsu.edu/math/faculty/watkins/

Structured eigenvalue methods for the computation of corner singularities in 3D anisotropic elastic structures

Thomas Apel* Volker Mehrmann† David Watkins‡

October 5, 2001

Abstract This paper is concerned with the computation of 3D vertex singularities of anisotropic elastic fields. The singularities are described by eigenpairs of a corresponding operator pencil on a subdomain of the sphere. The solution approach is to introduce a modified quadratic variational boundary eigenvalue problem which consists of two self-adjoint, positive definite sesquilinear forms and a skew-Hermitian form. This eigenvalue problem is discretized by the finite element method. The resulting quadratic matrix eigenvalue problem is then solved with the Skew Hamiltonian Implicitly Restarted Arnoldi method (SHIRA) which is specifically adapted to the structure of this problem. Some numerical examples are given that show the performance of this approach.

Key Words linear elasticity, Lamé equations, 3D vertex singularities, finite element methods, quadratic eigenvalue problems, Skew-Hamiltonian/Hamiltonian pencil, implicitly restarted Arnoldi method

AMS(MOS) subject classification 65N25; 65N30, 65F15, 74G70

1 Introduction

This paper is concerned with the study of the nature of three-dimensional elastic fields near the vertex of a polyhedron. It is well known that stress singularities can arise in a neighborhood of the vertex. The detailed knowledge of the singular terms of the elastic fields is of interest e.g. in crack mechanics, where the intersection of crack fronts or notches with the surface of the body generates vertices. Moreover, in computational mechanics, the lack of regularity near edges or corners demands modified discretization procedures. Our goal is to describe a mathematical method that leads to an efficient computation of the vertex singularities and to demonstrate the features of the new approach via several numerical examples.

*Supported by Deutsche Forschungsgemeinschaft within SFB 393.

†Supported by Deutsche Forschungsgemeinschaft within Project Me12-1

‡Most of this author's work was performed while visiting TU Chemnitz.

The key feature of the new approach is the interplay between the mathematical modelling and the analysis of the structure of the model with the numerical methods specifically designed for the efficient and accurate solution of the resulting quadratic eigenvalue problem.

We will briefly recall in Section 2 how the linear elasticity problem for isotropic and even anisotropic materials in a polyhedral domain under the action of body and surface forces leads to a quadratic operator eigenvalue problem of the form

$$\lambda^2 m(u,v) + \lambda g(u,v) - k(u,v) = 0, \tag{1}$$

where m, k are Hermitian forms and g is a skew Hermitian form. Spectral properties of such eigenvalue problems have been studied for the Lamé system, for example, in [15, 17, 19], see also [18] and the literature cited therein. Numerical solution techniques with a boundary element method on graded meshes and a boundary integral method are developed in [31, 34] and [9], respectively. A finite element approach similar to ours is described and used in [2, 8, 21]. There are many papers concerning the computation of corner singularities of plane elasticity problems and of rotationally-symmetric three-dimensional problems which are much simpler and shall therefore not be reviewed here.

In Section 3, we briefly recall from [1] the construction of a finite element method with piecewise linear basis functions on graded meshes that produces second order accurate approximate eigenvalues. This method leads to a quadratic matrix eigenvalue problem of the form

$$(\lambda^2 M + \lambda G - K)u = 0. \tag{2}$$

Numerical methods for quadratic eigenvalue problems have recently received a renewed interest, due to many important applications, see [23, 24] for recent surveys. The solution of quadratic eigenvalue problems is typically done via a linearization procedure, where the quadratic problem is embedded into a double size linear generalized eigenvalue problem. Apart from the doubling of the dimension there are other disadvantages to this linearization procedure, like the increase of the condition number of the problem, i.e., the linearized system is sometimes much more sensitive to perturbations in the data than the original problem, see [33]. On the other hand there are no efficient methods known that work directly with the quadratic eigenvalue problem. Furthermore, it was observed in [21, 27] that the eigenvalue problems (1) and (2) have a specific symmetry structure in the spectrum. Similar structures arise also in other applications, see [24].

For an efficient and accurate procedure it is essential to reflect the structure of the problem also in the numerical method to solve the algebraic eigenvalue problem. Such a method has been suggested recently in [27] and we demonstrate in Section 4 the use of this new approach in the context of the elasticity problem. Implementation details are described in Section 5. From several test series we document two in Section 6. With this we show the efficiency of the method.

2 Setting of the problem

Consider the linear elasticity problem in a polyhedral domain Ω^{3D} under the action of body and surface forces $f = [f_i]_{i=1}^3$ and $g = [g_i]_{i=1}^3$, respectively. The elastic stiffness coefficients a_{ijkl} satisfy the classical symmetry and positivity relations,

$$a_{ijkl} = a_{klij} = a_{jikl} = a_{ijlk}, \qquad \sum_{i,j,k,l=1}^{3} a_{ijkl}\xi_{ij}\xi_{kl} \geq \alpha \sum_{i,j=1}^{3} \xi_{ij}^2 \quad \forall \xi_{ij} \in \mathbb{R},$$

even when the material is anisotropic. We assume that the coefficients are piecewise constant, which means that the material is piecewise homogeneous but can be composite. Using the notation $U = [U_i]_{i=1}^3$ for the displacement field and $\varepsilon_{ij}(U) = \frac{1}{2}(\partial_i u_j + \partial_j u_i)$, $i, j = 1, 2, 3$, for the components of the corresponding linearized strain tensor, the linear elasticity problem is described in variational (weak) form by

$$\sum_{i,j,k,l=1}^{3} \int_{\Omega^{3D}} a_{ijkl}\varepsilon_{ij}(U)\varepsilon_{kl}(V) = \int_{\Omega^{3D}} f_i V_i + \int_{\Gamma_2^{3D}} g_i V_i \quad \forall V \in V_0^{3D},$$

where $V_0^{3D} = \{V \in H^1(\Omega^{3D})^3 : V = 0 \text{ on } \Gamma_1^{3D}\}$ is the space of admissible displacement fields.

It is well known, see for example the fundamental work [14], research articles as [11, 19, 17], the monographs [5, 10, 16, 18, 20] and the vast literature cited therein, that the singular terms of the elastic field near a vertex have the asymptotic form (here written without logarithmic terms)

$$\sum_i c_i r^{\alpha_i} u^{(i)}(\varphi, \theta),$$

where α_i are the eigenvalues and $u^{(i)}$ are the eigenfunctions of a quadratic eigenvalue problem and (r, φ, θ) are spherical coordinates centered in the vertex of interest. This eigenvalue problem is derived, e.g., in [21] and has the form

$$0 = -\alpha(\alpha+1)\, a(u, v) - (\alpha+1)\, b(u, v) + \alpha\, c(u, v) + d(u, v) \quad \forall v \in V_0, \tag{3}$$

with an appropriate complex Hilbert space V_0. For its definition we assume that in a neighborhood of the vertex the three-dimensional domain Ω^{3D} can be described by

$$\Omega^{3D} := \{(r\cos\varphi\sin\theta, r\sin\varphi\sin\theta, r\cos\theta) \in \mathbb{R}^3 :\ 0 < r < r_0,\ (\varphi, \theta) \in \Omega\}.$$

The intersection of Ω^{3D} with the unit sphere S^2 is therefore

$$\tilde{\Omega} := \Omega^{3D} \cap S^2 = \{(\cos\varphi\sin\theta, \sin\varphi\sin\theta, \cos\theta) \in \mathbb{R}^3 :\ (\varphi, \theta) \in \Omega\}.$$

Similarly we define $\tilde{\Gamma}_1 := \Gamma_1^{3D} \cap S^2$. Using the isomorphism $\Omega \leftrightarrow \tilde{\Omega}$ we define the space $V_0 := \{v : \tilde{v} \in \tilde{V}_0\}$ with $\tilde{V}_0 := \{\tilde{v} \in H^1(\tilde{\Omega}) : \tilde{v} = 0 \text{ on } \tilde{\Gamma}_1\}$.

For the definition of the sesquilinear forms in (3) we define vector functions A, B, C, such that $\nabla U = A\partial_r U + B\,\frac{1}{r}\partial_\theta U + C\,\frac{1}{r}\partial_\varphi U$,

$$\begin{array}{lll} A_1 = \cos\varphi\sin\theta, & B_1 = \cos\varphi\cos\theta, & C_1 = -\sin\varphi/\sin\theta, \\ A_2 = \sin\varphi\sin\theta, & B_2 = \sin\varphi\cos\theta, & C_2 = \cos\varphi/\sin\theta, \\ A_3 = \cos\theta, & B_3 = -\sin\theta, & C_3 = 0, \end{array}$$

and we use the abbreviations

$$s_j(u_i) = A_j u_i, \qquad e_j(u_i) = -\frac{1}{2}A_j u_i + B_j\partial_\theta u_i + C_j\partial_\varphi u_i,$$

and $\mathrm{d}\omega = \sin\theta\,\mathrm{d}\theta\mathrm{d}\varphi$. The forms are then given by

$$\begin{aligned} a(u,v) &= \sum_{i,j,k,l=1}^{3}\int_\Omega a_{ijkl}\; s_j(u_i)\; s_l(\overline{v}_k)\,\mathrm{d}\omega, \\ b(u,v) &= \sum_{i,j,k,l=1}^{3}\int_\Omega a_{ijkl}\; [e_j(u_i) + \tfrac{1}{2}s_j(u_i)]\; s_l(\overline{v}_k)\,\mathrm{d}\omega, \\ c(u,v) &= \sum_{i,j,k,l=1}^{3}\int_\Omega a_{ijkl}\; s_j(u_i)\; [e_l(\overline{v}_k) + \tfrac{1}{2}s_l(\overline{v}_k)]\,\mathrm{d}\omega \;=\; \overline{b(v,u)}, \\ d(u,v) &= \sum_{i,j,k,l=1}^{3}\int_\Omega a_{ijkl}\; [e_j(u_i) + \tfrac{1}{2}s_j(u_i)]\; [e_l(\overline{v}_k) + \tfrac{1}{2}s_l(\overline{v}_k)]\,\mathrm{d}\omega. \end{aligned}$$

By changing the parameter α to $\lambda = \alpha + 1/2$ the eigenvalue problem (3) can be written as

$$\lambda^2 m(u,v) + \lambda g(u,v) - k(u,v) = 0, \tag{4}$$

with sesquilinear forms

$$\begin{aligned} m(u,v) &= \sum_{i,j,k,l=1}^{3}\int_\Omega a_{ijkl}\; s_j(u_i)\; s_l(\overline{v}_k)\,\mathrm{d}\omega, \\ g(u,v) &= \sum_{i,j,k,l=1}^{3}\int_\Omega a_{ijkl}\; [e_j(u_i)\; s_l(\overline{v}_k) - s_j(u_i)\; e_l(\overline{v}_k)]\,\mathrm{d}\omega, \\ k(u,v) &= \sum_{i,j,k,l=1}^{3}\int_\Omega a_{ijkl}\; e_j(u_i)\; e_l(\overline{v}_k)\,\mathrm{d}\omega. \end{aligned}$$

The advantage of rewriting the system in this form is that these sesquilinear forms have nice symmetry properties, namely

$$\begin{aligned} m(u,v) &= \overline{m(v,u)}, \\ g(u,v) &= -\overline{g(v,u)}, \\ k(u,v) &= \overline{k(v,u)}. \end{aligned}$$

Due to these symmetries we also have a symmetry in the spectrum.

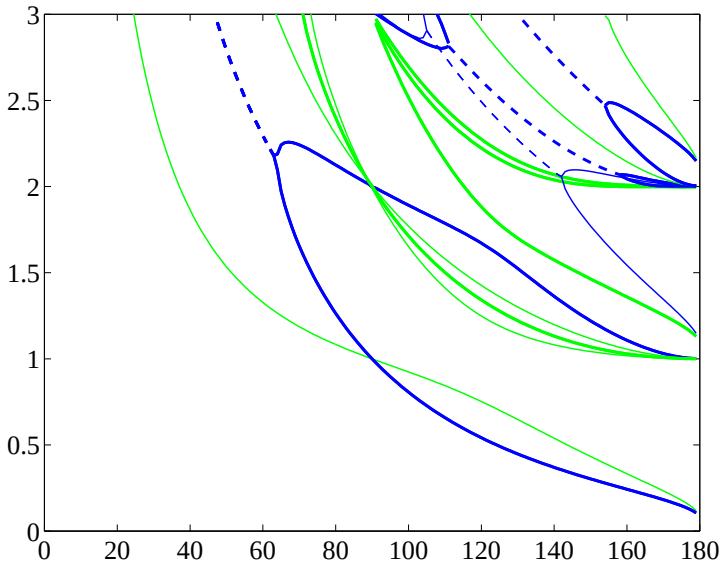

Figure 1: Real part of the eigenvalues α with $\operatorname{Re}\alpha \in [0,3]$ for the Dirichlet problem in a circular cone with opening angle ξ; numerical calculations with mesh parameter $h = 3^\circ = \pi/60 \approx 0.052$

Proposition 1 *[27] If λ is an eigenvalue of (4), then also $-\lambda$ is an eigenvalue. If λ is not real, then $\overline{\lambda}$ and $-\overline{\lambda}$ are also eigenvalues, so the eigenvalues come in quadruples.*

We remark that such symmetry results were known previously both in the analysis community, see e. g. [18, Thm. 11.3.1], and in the engineering community, see e. g. [21].

In our application we are interested in few eigenvalues (and eigenvectors) nearest to the imaginary axis. As an example, Figure 1 displays the real part of all approximated eigenvalues α with real part in the interval $[0,3]$ for the corner of a circular cone with opening angle ξ. For simplicity in this example we have considered an isotropic material with Poisson ratio $\nu = 0.3$. We display the eigenvalues α of problem (3) instead of λ since the former are originally sought and the latter were introduced only to simplify the mathematical model. We see lines of simple (thin) and double (thick) eigenvalues which can be real (solid) or complex (dashed). We also observe points where two or more eigenvalue curves cross (*crossing points*), and points where two real eigenvalues become a pair of complex conjugate eigenvalues (*bifurcation points*).

Apart from the computation of the eigenvalues themselves it is also an important problem to determine the crossing and bifurcation points. In particular, eigenvalues with a geometric multiplicity that differs from the algebraic multiplicity lead to instabilities of the asymptotic expansion of the displacement field, known as the Sternberg–Koiter paradox, see [30] and the references therein.

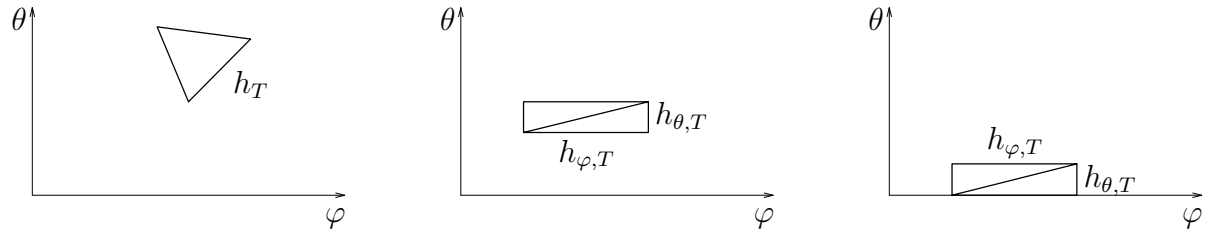

Figure 2: Illustration of different cases of triangles

3 The discretized eigenvalue problem

For the numerical solution of the continuous eigenvalue problem we construct a finite element subspace $V_{0h} \subset V_0$ and look for the finite element solutions of problem (4), i.e., for $\lambda_h \in \mathbb{C}$ and $u_h \in V_{0h} \setminus \{0\}$ such that

$$\lambda_h^2 \, m(u_h, v_h) + \lambda_h \, g(u_h, v_h) - k(u_h, v_h) = 0 \quad \forall v_h \in V_{0h}. \tag{5}$$

In our case, the space V_{0h} is defined by the set of continuous functions from V_0 which are piecewise linear on a triangular finite element mesh $\mathcal{T}_h$. This approach to solve the problem is widely used in the engineering literature, see, e. g., [21, 32].

In order to describe the meshes we make the simplifying assumption that the domain Ω is polygonal. Note that Ω is not uniquely defined; in particular, we have the freedom to choose the north pole appropriately. We consider a family of meshes $\mathcal{T}_h = \{T\}$ with the usual admissibility conditions: We assume that $\overline{\Omega} = \bigcup_{T \in \mathcal{T}_h} \overline{T}$ where the elements T are mutually disjoint open triangles. Any side of any triangle T is either part of the boundary $\partial\Omega$ or side of another triangle $T' \in \mathcal{T}_h$. For each triangle we define the number $\theta_{-,T} := \inf_{(\varphi,\theta)\in T} \sin\theta$.

Concerning the shape of the elements, we distinguish two cases and make the following assumption. For triangles T with $\theta_{-,T} \geq \theta_* = \text{const.} > 0$ we assume that T has bounded aspect ratio, without further constraints. The diameter of T is denoted by h_T. For an illustration see Figure 2, left hand side. In the second case, when $\theta_{-,T} < \theta_*$, we assume that two edges of T are parallel to the coordinate axes. Their lengths are denoted by $h_{\varphi,T}$ and $h_{\theta,T}$ which can be chosen independently, see also Figure 2, middle and right. That means the aspect ratio of T may not be bounded by a constant.

If $\tilde{\Omega}$ is a smooth domain then the eigenfunctions are regular and no local mesh refinement is needed for their approximation. This means $h_T \sim h$ for all $T \in \mathcal{T}_h$, and the aspect ratio of all elements is bounded.

However, the eigenfunctions have, in general, singularities near corners of $\tilde{\Omega}$ or near points of $\partial\tilde{\Omega}$ where the boundary conditions change their type, in the following also referred to as corners. Therefore, it was suggested in [1] to use refined meshes in these critical regions. For their description we need some further notation and distinguish two cases. Let the corner be denoted by $P = (\varphi_0, \theta_0)$ in the parameter plane. Determine a lower estimate $\tilde{\alpha}$ for the leading singularity exponent α of the edge created by the corner P, e. g. $\tilde{\alpha} = 0.5$ for the Dirichlet problem. Choose a parameter $\beta \in (1-\alpha, 1)$, e. g. $\beta = 1 - \tilde{\alpha}$.

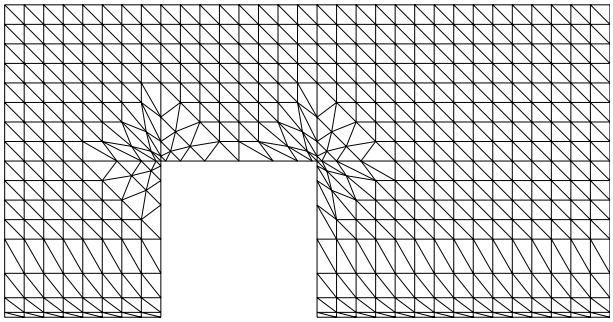

Figure 3: Graded mesh for the Fichera example.

Case 1, $\theta_0 \notin \{0, \pi\}$**:** The aspect ratio of the elements is bounded and

$$h_T \sim \begin{cases} h^{1/(1-\beta)} & \text{if } \operatorname{dist}(P,T) = 0, \\ h\,[\operatorname{dist}(P,T)]^{\beta} & \text{if } \operatorname{dist}(P,T) > 0. \end{cases}$$

This means that $h_T \sim h$ for $\operatorname{dist}(P,T) > C_* = \text{const}$.

Case 2, $\theta_0 \in \{0, \pi\}$**:** The refinement zone is determined by $\sin\theta < \theta_*$. The elements might be anisotropic,

$$h_{\varphi,T} \sim h, \qquad h_{\theta,T} \sim \begin{cases} h^{1/(1-\beta)} & \text{if } \theta_{-,T} = 0, \\ h\,\theta_{-,T}^{\beta} & \text{if } \theta_{-,T} > 0. \end{cases}$$

In Figure 3, we display a mesh which was used in [1] and below in Section 6 for the well-known Fichera corner domain.

The following approximation results are formulated for meshes defined by the rules above.

Proposition 2 *Consider an eigenpair (λ, u) of (4) and denote by κ the maximal size of an associated Jordan block. For a sequence of eigenpairs $\{(\lambda_h, u_h)\}_{h\to 0}$ with $\lambda_h \to \lambda_0$ the estimates*

$$\begin{aligned} |\lambda_0 - \lambda_h| &\le Ch^{2/\kappa}, \\ \|u_0 - u_h\|_V &\le Ch^{\alpha}, \quad \alpha = \min\{1, 2/\kappa\} \end{aligned}$$

hold.

According to [13] the convergence rate can be improved for $\kappa > 1$ by averaging.

Proposition 3 *For an eigenvalue λ_0 with algebraic multiplicity m there exist m disjoint sequences $\{\lambda_{h,i}\}$ with $\lambda_{h,i} \to \lambda_0$, $i = 1, \ldots, m$. Then for the arithmetic mean $\hat{\lambda}_h := \frac{1}{m}\sum_{i=1}^{m} \lambda_{h,i}$ the improved estimate*

$$|\lambda_0 - \hat{\lambda}_h| \le Ch^2$$

holds.

These propositions were proved in [1] for the Dirichlet problem. Anisotropic materials are included. Other boundary conditions can be treated in a similar way. Composite materials are also included if the subdomains with different material properties can be resolved by the finite element mesh.

4 The algebraic eigenvalue problem

The quadratic eigenvalue problem (5) is equivalent to a quadratic matrix eigenvalue problem in the space $\mathbb{R}^N$, $N = \dim V_{0h}$: Find $\lambda \in \mathbb{C}$, $\underline{u} \in \mathbb{R}^N \setminus \{\underline{0}\}$ such that

$$(\lambda^2 M + \lambda G - K)\underline{u} = 0. \tag{6}$$

As we have already indicated, this problem has considerable structure, and one should use methods that exploit this structure.

From the properties of the sesquilinear form it follows that

$$M = M^T > 0, \quad G = -G^T, \quad K = K^T > 0,$$

so we need to store only the upper triangle part of each matrix. The symmetries also imply the eigenvalue symmetry in Proposition 1. Therefore, if we have a method to solve eigenvalue problem that does not disturb this symmetry, only a fraction of about one quarter to one half of the eigenvalues needs to be approximated. Furthermore, methods that respect the structure tend to be more stable and accurate than methods that do not. This has been shown for small problems with the given eigensymmetry in [4]. Finally, the matrices M, K, and G are large sparse finite element matrices. That means that the multiplication of such a matrix by a vector is a cheap operation, much cheaper (with respect to time and memory) than, for example, a matrix factorization.

The standard approach for solving quadratic eigenvalue problems is to make an appropriate linearization. Simple linearizations are obtained by setting $\underline{v} = \lambda\underline{u}$, for example,

$$\begin{bmatrix} O & I \\ K & -G \end{bmatrix} \begin{bmatrix} \underline{u} \\ \underline{v} \end{bmatrix} = \lambda \begin{bmatrix} I & O \\ O & M \end{bmatrix} \begin{bmatrix} \underline{u} \\ \underline{v} \end{bmatrix},$$

$$\begin{bmatrix} O & I \\ K & O \end{bmatrix} \begin{bmatrix} \underline{u} \\ \underline{v} \end{bmatrix} = \lambda \begin{bmatrix} I & O \\ G & M \end{bmatrix} \begin{bmatrix} \underline{u} \\ \underline{v} \end{bmatrix}.$$

However, these linearizations do not preserve the structure. Following [27] we set $\underline{v} = \lambda M\underline{u}$ and use the linearization

$$\lambda \begin{bmatrix} I & G \\ O & I \end{bmatrix} \begin{bmatrix} \underline{v} \\ \underline{u} \end{bmatrix} = \begin{bmatrix} O & K \\ M^{-1} & O \end{bmatrix} \begin{bmatrix} \underline{v} \\ \underline{u} \end{bmatrix}.$$

Introducing the matrices

$$B = \begin{bmatrix} I & G \\ O & I \end{bmatrix}, \qquad A = \begin{bmatrix} O & K \\ M^{-1} & O \end{bmatrix}, \qquad J = \begin{bmatrix} O & I \\ -I & O \end{bmatrix},$$

we find that the matrix B is skew Hamiltonian, a property which is defined by $(JB)^T = -JB$, and the matrix A is Hamiltonian, defined by $(JA)^T = JA$, see [4, 25]. Therefore, the matrix pencil $\lambda B - A$ is called Skew-Hamiltonian Hamiltonian pencil, shortly SHH pencil. The properties of such pencils are studied in detail in [25, 26]. Every SHH pencil has the eigenvalue symmetry described in Proposition 1 and thus, this linearization has preserved an essential structural property.

We can perform some more transformations with the SHH pencil. The matrix B can be factorized by

$$B = \begin{bmatrix} I & G \\ O & I \end{bmatrix} = \begin{bmatrix} I & \frac{1}{2}G \\ O & I \end{bmatrix} \begin{bmatrix} I & \frac{1}{2}G \\ O & I \end{bmatrix} = Z^2,$$

see [3, 27] for factorizations of this kind. Thus the SHH pencil can be written as

$$\lambda B - A = Z(\lambda I - Z^{-1}AZ^{-1})Z = Z(\lambda I - H)Z$$

with $H = Z^{-1}AZ^{-1}$, where the matrix H is again Hamiltonian. Since

$$Z^{-1} = \begin{bmatrix} I & -\frac{1}{2}G \\ O & I \end{bmatrix},$$

we conclude that we are interested in the eigenvalues of the Hamiltonian matrix

$$H = \begin{bmatrix} I & -\frac{1}{2}G \\ O & I \end{bmatrix} \begin{bmatrix} O & K \\ M^{-1} & O \end{bmatrix} \begin{bmatrix} I & -\frac{1}{2}G \\ O & I \end{bmatrix}.$$

Iterative methods such as subspace iteration and the Arnoldi method are easy to apply to this Hamiltonian matrix, but they typically give the eigenvalues with largest moduli. In our application the eigenvalues of interest are the one with smallest real part, so it makes more sense to work with the inverted matrix

$$H^{-1} = \begin{bmatrix} I & \frac{1}{2}G \\ O & I \end{bmatrix} \begin{bmatrix} O & M \\ K^{-1} & O \end{bmatrix} \begin{bmatrix} I & \frac{1}{2}G \\ O & I \end{bmatrix},$$

which is also Hamiltonian. In the interest of faster convergence, it would be even better to shift the matrix and then invert. Thus one would work with the shifted, inverted matrix $(H - \tau I)^{-1}$, where τ is a shift value that targets the eigenvalues we are interested in. Unfortunately (but not surprisingly) the shift destroys the Hamiltonian structure. If we wish to find eigenvalues near $\tau \in \mathbb{R}$ while also preserving structure, we must simultaneously seek the eigenvalues near $-\tau$. Thus we should also use $-\tau$ as a shift. This suggests using the operator $(H - \tau I)^{-1}(H + \tau I)^{-1}$, which turns out to be skew Hamiltonian [27, Prop. 3.2]. If τ is not real, we should also use $\overline{\tau}$ and $-\overline{\tau}$ as targets. Thus we consider two cases,

$$C = \begin{cases} (H - \tau I)^{-1}(H + \tau I)^{-1} & \text{if } \tau \text{ is real,} \\ (H - \tau I)^{-1}(H + \tau I)^{-1}(H - \overline{\tau} I)^{-1}(H + \overline{\tau} I)^{-1} & \text{if } \tau \text{ is complex.} \end{cases} \tag{7}$$

In both cases C is real and skew Hamiltonian.

We have lost the Hamiltonian structure but gained a related structure, which can be exploited in the *Skew Hamiltonian Implicitly Restarted Arnoldi* method, SHIRA [27]. *Implicitly Restarted* means that the standard Arnoldi method is combined with a subspace iteration. The modification for skew Hamiltonian matrices consists of an additional orthogonalization step. Normally the Arnoldi process builds a set of orthonormal vectors $q_1, \ldots, q_k$. SHIRA does this too, but it also ensures that $Jq_1, \ldots, Jq_k$ are orthogonal to $q_1, \ldots, q_k$. This additional orthogonality condition, which is called *isotropy*, is satisfied automatically in theory if C is skew Hamiltonian. However, it is lost in practice due to roundoff errors, unless it is enforced explicitly. Explicit enforcement of isotropy is crucial to the efficiency of the method [27].

SHIRA is an iterative method that multiplies C by a vector in each iteration. The matrix C consists of factors of the type

$$\begin{aligned}(H-\sigma I)^{-1} &= (Z^{-1}AZ^{-1}-\sigma I)^{-1} = Z(A-\sigma B)^{-1}Z \qquad (B=Z^2)\\ &= \begin{bmatrix} I & \frac{1}{2}G+\sigma M \\ O & I \end{bmatrix}\begin{bmatrix} O & M \\ -Q(\sigma)^{-1} & O \end{bmatrix}\begin{bmatrix} I & \frac{1}{2}G+\sigma M \\ O & I \end{bmatrix} \qquad (8)\end{aligned}$$

with $Q(\sigma) = \sigma^2 M + \sigma G - K$. The expensive part of the application of the operator C is the solve with $Q(\sigma)$. This matrix is symmetric only for $\sigma = 0$ and real only for real σ. In general a sparse complex LU decomposition is necessary [27].

We note that one LU decomposition suffices for all factors of C since $Q(-\lambda) = Q(\lambda)^T$ and $Q(\overline{\lambda}) = \overline{Q(\lambda)}$. We note also that the method becomes particularly cheap in memory when $\tau = 0$ is sufficient for approximating the desired eigenvalues. In this case we can work with a Cholesky decomposition. In our numerical tests we have good experience with real shifts, so in the following we restrict ourselves to this case.

5 Programming details

The meshes were generated by using a collection of subroutines [29] written by Uwe Reichel, TU Chemnitz. The library allows easy generation of meshes when the domain is the union of rectangles. Special routines allow for mesh grading to special points or lines, and for the treatment of various types of boundary conditions including periodic ones.

The integrals in the definition of the matrix entries were approximated by a 7-point rule of algebraic order 5. The matrices were generated using libraries that have been maintained for many years by the Chemnitz numerics group [12]. The graphics tool was supplied by Matthias Pester [28].

The implementation of the SHIRA algorithm is based on the ARPACK package [22]. Only a slight modification is made to enforce isotropy, as discussed in Section 4.

To apply the operator C from (7) using the factorization (8), we have to solve systems with the sparse matrices $Q(\tau)$ and $Q(-\tau) = Q(\tau)^T$. For this we used version 1.1 of the package SuperLU [7]. We are doing also tests with version 2.2 of UMFPACK [6]. The computation time is comparable with that of SuperLU; in many cases UMFPACK is

slightly slower than SuperLU, but in some cases also quicker. In order to avoid confusion we report in Section 6 only the results with SuperLU.

For comparison purposes we also applied ARPACK to $(H - \tau I)^{-1}$. Again, we used version 1.1 of the package SuperLU for the factorization of $Q(\tau)$.

In all cases we used the Arnoldi method with a stopping tolerance of 10^{-12}.

It is well known that the convergence of the Arnoldi method will depend on the starting vector q_0. In one mode of the program we use a chaotic starting vector q_0. This means the entries of q_0 were generated by a random number generator with always the same seed. So we ensure a fair comparison by using in all tests the same q_0.

In the examples described below we are interested in solving several eigenvalue problems that differ only by a smoothly changing parameter. Therefore we expect continuously changing eigenvalues from one computation to the next. In order to exploit the results from the previous calculation we average all the Arnoldi vectors generated in the previous calculation. In a further mode of the program this vector is used as the starting vector in the next calculation.

All tests were carried out on a Linux machine with an 800 MHz Intel processor and 768 MByte RAM.

6 Numerical Results

We tested the algorithms with the following two examples.

Example 1 (Fichera corner) The three-dimensional domain Ω^{3D} can be described as a cube from which a cube of smaller size has been removed. A representation of Ω in the parameter plane is shown in Figure 3. This problem has been considered in the literature for isotropic material, for example in [31] for a single material and Dirichlet boundary conditions and in [8] for a bi-material joint and Neumann boundary conditions. Our tests are similar to those in the latter reference.

The material is defined by

$$\nu = 0.3, \qquad E = \begin{cases} E_1 = 1.0 & \text{for } \theta < \frac{1}{2}\pi, \\ E_2 & \text{for } \theta > \frac{1}{2}\pi, \end{cases}$$

where E_2 is varied in the interval $[0.016, 64]$. These values of E do not describe particular materials but the eigenvalues depend only on ν and the ratio of E_1 and E_2.

The pure Neumann problem has three eigenvalues $\alpha = 0$ (rigid body translation) and three eigenvalues $\alpha = 1$ (rigid body rotation). The eigenvalues of interest are those five in between since they create the singularities in the displacement. They are plotted against E_2 in Figure 4. With this example we have shown that we can accomplish parameter studies with composite materials.

Example 2 (Crack) We consider a halfspace with a crack intersecting the surface. In the parameter plane we can use

$$\Omega = \{(\phi, \theta) : \phi \in (0, \pi), \theta \in (0, \pi)\} \setminus \{(\phi, \theta) : \phi = \xi, \theta \in (0, \tfrac{1}{2}\pi]\},$$

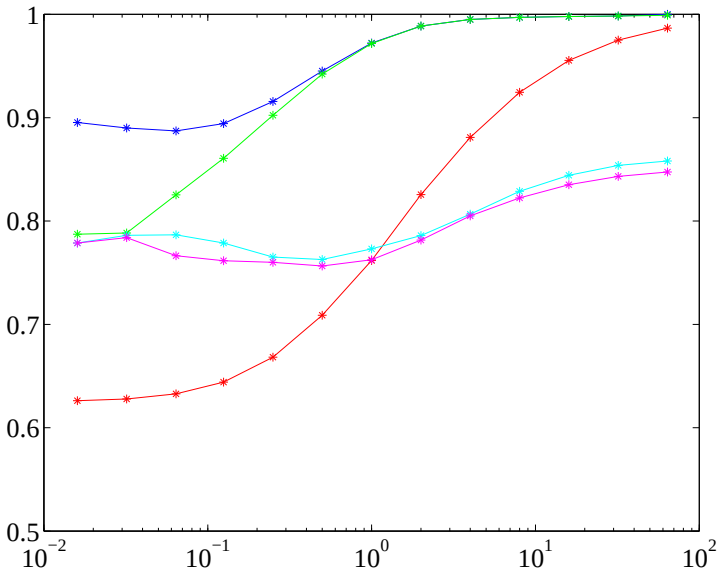

Figure 4: Fichera example: Eigenvalues $\alpha \in (0, 1)$ for various material parameters, calculated with $h = \pi/128 \approx 0.025$

see Figure 5 for an illustration. At a workshop held in Chemnitz in April 2000 this problem was suggested as the most challenging of four benchmark examples for computing singularity exponents. In our tests we used isotropic material with $\nu = 0.3$ and $E = 1$ (in the uni-material case the eigenvalues do not depend on E) and computed the eigenvalues for varying angle $\xi \in (0, \frac{1}{2}\pi] = (0°, 90°]$.

As in example 1 we investigated the case of pure Neumann boundary conditions. Therefore we have triple eigenvalues $\alpha = 0$ and $\alpha = 1$, see the thick lines in Figure 6. All further integers are also multiple eigenvalues. Moreover, we found three single real eigenvalues $\alpha \in (0, 1)$ where one of them is very close to one. Since the distribution of the eigenvalues in the interval $(1, 2)$ is much more attractive, we computed them as well. Again, dashed lines indicate eigenvalues with nonzero imaginary part. Example 2 shows that we can treat cracks.

Figure 7 shows the time for computing the smallest 15 eigenvalues, those in the interval $[0, 2)$, with different versions of the solver. The dimension of the matrices K, G and M is 43383. The time includes the assembly of the matrices, LU-factorization of $Q(\tau)$ and the Arnoldi iteration. Eigenvectors are not computed. For each angle the iteration started with the same chaotic vector which makes the computation time comparable. We compare SHIRA (solid lines) with a standard shift-and-invert implicitly restarted Arnoldi method (IRA, dashed lines).

The advantage of SHIRA can be seen best when comparing the case with the shift $\tau = 0$ (diagrams on the left hand side). While SHIRA computes only the desired 15 eigenvalues, IRA computes also the uninteresting eigenvalues $-\lambda$, so we have to solve for 30 eigenvalues

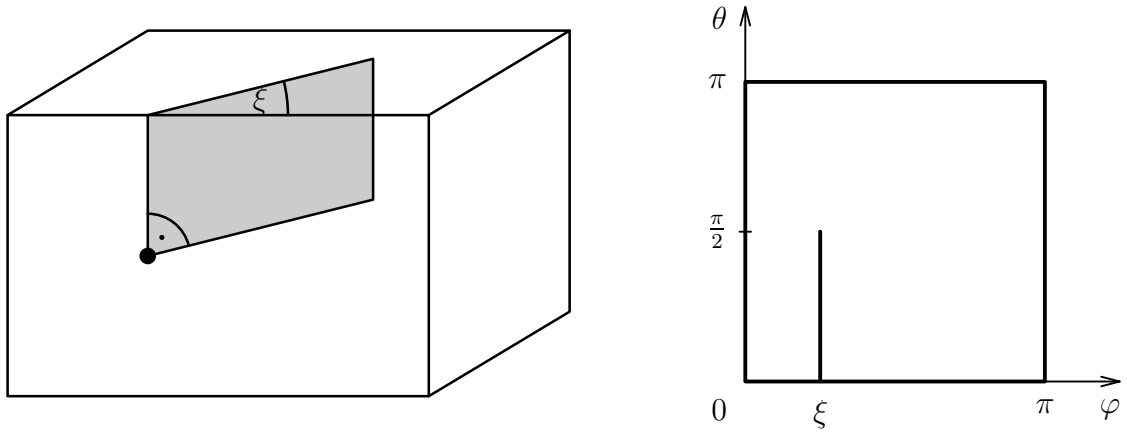

Figure 5: Illustration of part of the three-dimensional crack domain (left) and of the corresponding two-dimensional domain in the parameter space (right)

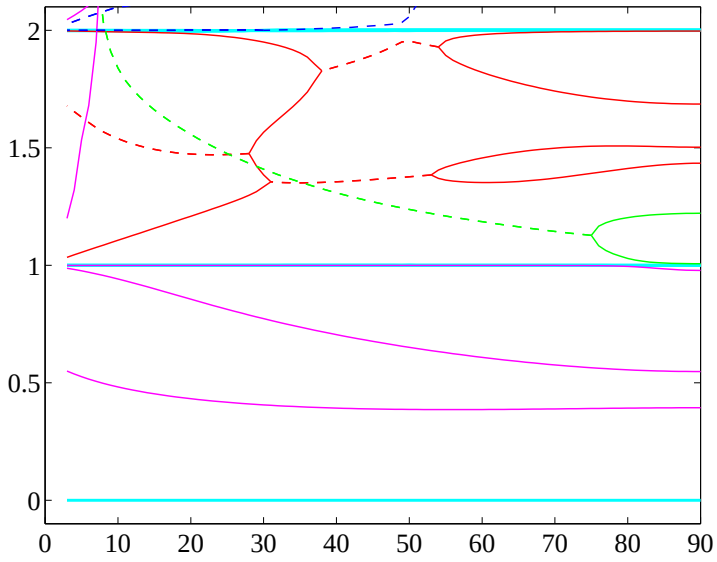

Figure 6: Crack example: Real part of eigenvalues α with $\operatorname{Re}\alpha \in (-0.1, 2.1)$ for various angles, calculated with $h = 1.5^\circ = \pi/120 \approx 0.026$; dashed lines for eigenvalues with $\operatorname{Im}\alpha \neq 0$

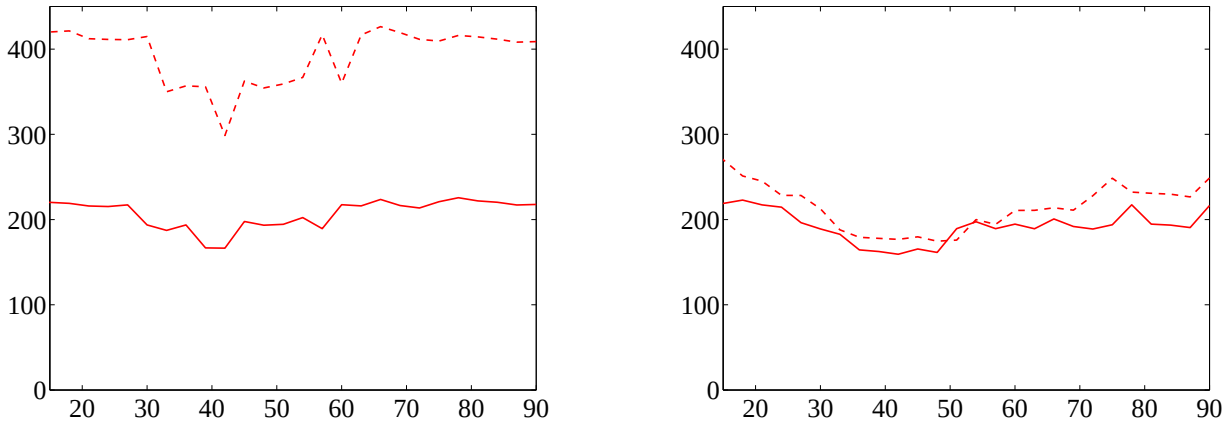

Figure 7: Crack example: Computing time in seconds for 15 eigenvalues in $[0, 2)$, calculated with $h = \pi/120$ and chaotic starting vector; solid lines: SHIRA, dashed lines: IRA with $(H - \tau I)^{-1}$; left: $\tau = 0$, right: $\tau = 1$

in order to get the 15 desired ones, which is much more expensive.

For an appropriately chosen shift value τ, for example $\tau = 1$, we need to compute with IRA only 15 eigenvalues, too. Then we find comparable computing times for SHIRA and IRA, with a small advantage for SHIRA. Note that the shift value $\tau = 1.5$ is too large, the (wanted) eigenvalues $\alpha = 0$ (i. e. $\lambda = 0.5$) have the same distance as the (not wanted) eigenvalues $\alpha = 2$ (i. e. $\lambda = 2.5$). Also, shifts $\tau < 1$ lead IRA to the calculation to compute negative eigenvalues $\alpha = -1$ (i. e. $\lambda = -0.5$).

To summarize, if we have a good shift, that is, if we have good advance knowledge of where the eigenvalues of interest lie, then IRA performs nearly as well as SHIRA. However, if we do not have a good shift, SHIRA will obtain the desired eigenvalues much more quickly than IRA does. Notice that SHIRA, unlike IRA, is relatively insensitive to the choice of shift. Although the flop counts reported in [27] indicate much lower complexity for SHIRA compared to IRA when the shift parameter is not chosen well, the runtimes of the Fortran/C implementation of the two methods are often not that different.

The computing time depends also on the parameter ξ. A minimum is achieved near $40°$ where the 15-th eigenvalue is best separated from the 16-th, which is $\alpha = 2$.

In the tests we have seen that the eigenvalues are identical up to 10 digits. The stabilizing effect of SHIRA seems to be unnecessary for this kind of application.

We hoped to save computing time by using a linear combination of the Arnoldi vectors of previous calculations to initialize the eigensolver, since the eigenpairs depend continously on the parameter. The potential of this method can be seen in the savings of about 30–40% when an example is calculated a second time. But the savings reduce to 15–20% when the parameter ξ is changed by $0.001°$. However, a change of ξ by $0.01°$ produces a computing time comparable with that using a chaotic starting vector. The situation improves slightly when we search only for the two well separated eigenvalues $\alpha \in (0, 1)$ but still savings can only be obtained when the parameter changes in impractically small steps.

7 Conclusions

We have developed codes to compute 3D vertex singularities of anisotropic elastic fields. The singularities are described by eigenpairs of an operator pencil on a subdomain of the sphere. We solved the problem by introducing a quadratic variational boundary eigenvalue problem which consists of two self-adjoint, positive definite sesquilinear forms and a skew-Hermitian form. This eigenvalue problem was then discretized by the finite element method. Finally, the resulting quadratic matrix eigenvalue problem was solved with the Skew Hamiltonian Implicitly Restarted Arnoldi method (SHIRA), which preserves and exploits the structure of this problem. Numerical results show that SHIRA is more efficient than a competing method that ignores the structure, particularly in situations when a good target shift for the eigenvalues is not known in advance.

Acknowledgement. The major work in coding the algorithms was done by Cornelia Pester, Uwe Reichel, and Maharavo Randrianarivony, all from TU Chemnitz, Germany. This help is gratefully acknowledged.

References

[1] Th. Apel, A.-M. Sändig, and S. I. Solov'ev. Error estimates for the computation of 3D vertex singularities for linear elasticity by a finite element method on graded meshes. In preparation.

[2] Z. P. Bažant and L. F. Estenssoro. Surface singularity and crack propagation. *Internat. J. Solids Structures*, 15:405–426, 1979.

[3] P. Benner, R. Byers, H. Faßbender, V. Mehrmann, and D. Watkins. Cholesky-like factorizations of skew-symmetric matrices. *ETNA*, 11:85–93, 2000.

[4] P. Benner, R. Byers, V. Mehrmann, and H. Xu. Numerical computation of deflating subspaces of embedded Hamiltonian pencils. Preprint SFB393/99-15, TU Chemnitz, 1999. Submitted to SIAM J. Matrix Anal. Appl.

[5] M. Dauge. *Elliptic boundary value problems on corner domains – smoothness and asymptotics of solutions*, volume 1341 of *Lecture Notes in Mathematics*. Springer, Berlin, 1988.

[6] T. A. Davis. *UMFPACK Version 3.0 User Guide*. Dept. of Computer and Information Science and Engineering, Univ. of Florida, Gainesville, FL, 2001.

[7] J. W. Demmel, J. R. Gilbert, and X. S. Li. SuperLU Users' Guide. Technical Report LBNL-44289, Lawrence Berkeley National Laboratory, 1999.

[8] A. Dimitrov, H. Andrä, and E. Schnack. Efficient computation of order and mode of corner singularities in 3d-elasticity. *Internat. J. Numer. Methods Engrg.*, 2001.

[9] E. V. Glushkov, N. V. Glushkova, and O. N. Lapina. 3D elastic stress singularity at polyhedral corner points. *Int. J. Solids Struct.*, 36:1105–1128, 1999.

[10] P. Grisvard. *Elliptic problems in nonsmooth domains*, volume 21 of *Monographs and Studies in Mathematics*. Pitman, Boston–London–Melbourne, 1985.

[11] P. Grisvard. Singularité en elasticité. *Archive for Rational Mechanics*, 107:157–180, 1989.

[12] G. Haase, Th. Hommel, A. Meyer, and M. Pester. Bibliotheken zur Entwicklung paralleler Algorithmen. Preprint SPC95_20, TU Chemnitz–Zwickau, 1995. Updated version of SPC94_4 and SPC93_1.

[13] O. O. Karma. Approximation in eigenvalue problems for holomorphic Fredholm operator functions. II: Convergence rate. *Numer. Funct. Anal. Optimization*, 17:389–408, 1996.

[14] V. A. Kondrat'ev. Boundary value problems for elliptic equations on domains with conical or angular points. *Trudy Moskov. Mat. Obshch.*, 16:209–292, 1967. In Russian.

[15] V. A. Kozlov and V. G. Maz'ya. Spectral properties of operator pencils, generated through elliptic boundary value problems in a cone. *Funkcionalniĭ analis i ego priloshenija*, 2:38–46, 1988. In Russian.

[16] V. A. Kozlov, V. G. Maz'ya, and J. Roßmann. *Elliptic Boundary Value Problems in Domains with Point Singularities*. American Mathematical Society, 1997.

[17] V. A. Kozlov, V. G. Maz'ya, and J. Roßmann. Spectral properties of operator pencils generated by elliptic boundary value problems for the Lamé system. *Rostocker Math. Kolloq.*, 51:5–24, 1997.

[18] V. A. Kozlov, V. G. Maz'ya, and J. Roßmann. *Spectral Problems Associated with Corner Singularities of Solutions to Elliptic Equations*. American Mathematical Society, 2001.

[19] V. A. Kozlov, V. G. Maz'ya, and C. Schwab. On singularities of solutions of the displacement problem of linear elasticity near the vertex of a cone. *Arch. Ration. Mech. Anal.*, 119:197–227, 1992.

[20] A. Kufner and A.-M. Sändig. *Some Applications of Weighted Sobolev Spaces*. Teubner, Leipzig, 1987.

[21] D. Leguillon. Computation of 3D-singularities in elasticity. In M. Costabel et al., editor, *Boundary value problems and integral equations in nonsmooth domains*, volume 167 of *Lect. Notes Pure Appl. Math.*, pages 161–170, New York, 1995. Marcel Dekker. Proceedings of a conference at CIRM, Luminy, France, May 3-7, 1993.

[22] R. B. Lehoucq, D. C. Sorensen, and C. Yang. *ARPACK user's guide. Solution of large-scale eigenvalue problems with implicitly restarted Arnoldi methods*, volume 6 of *Software - Environments - Tools*. SIAM, Philadelphia, PA, 1998.

[23] K. Meerbergen. Locking and restarting quadratic eigenvalue solvers. *SIAM J. Sci. Comput.*, 22:1814–1839, 2001.

[24] K. Meerbergen and F. Tisseur. The quadratic eigenvalue problem. *SIAM Review*, 43:235–286, 2001.

[25] C. Mehl. *Compatible Lie and Jordan algebras and applications to structured matrices and pencils*. PhD thesis, TU Chemnitz, 1998.

[26] C. Mehl. Condensed forms for skew-Hamiltonian/Hamiltonian pencils. *SIAM J. Matrix Anal. Appl.*, 21:454–476, 1999.

[27] V. Mehrmann and D. Watkins. Structure-preserving methods for computing eigenpairs of large sparse skew-Hamiltonian/Hamiltonian pencils. *SIAM J. Sci. Comp.*, 22:1905–1925, 2001.

[28] M. Pester. Grafik-Ausgabe vom Parallelrechner für 2D-Gebiete. Preprint SPC94_24, TU Chemnitz-Zwickau, 1994.

[29] U. Reichel. *NetMake – C-Subroutinensammlung zur Netzgenerierung*. TU Chemnitz, Fak. f. Mathematik, 1999.

[30] A. Rössle and A.-M. Sändig. Stress singularities in bonded dissimilar materials under mechanical and thermal loading. *Computational Materials Science*, 7:48–55, 1996.

[31] H. Schmitz, K. Volk, and W. L. Wendland. On three-dimensional singularities of elastic fields near vertices. *Numer. Methods Partial Differential Equations*, 9:323–337, 1993.

[32] V. Staroverov, G. Kobelkov, E. Schnack, and A. Dimitrov. On numerical methods for flat crack propagation. IMF-Preprint 99-2, Universität Karlsruhe, 1999.

[33] F. Tisseur. Stability of structured Hamiltonian eigensolvers. *SIAM J. Matrix Anal. Appl.*, 23:103–125, 2001.

[34] K. Volk. *Zur Berechnung von Singulärfunktionen dreidimensionaler elastischer Felder*. PhD thesis, Universität Stuttgart, 1989.

Other titles in the SFB393 series:

01-01 G. Kunert. Robust local problem error estimation for a singularly perturbed problem on anisotropic finite element meshes. January 2001.

01-02 G. Kunert. A note on the energy norm for a singularly perturbed model problem. January 2001.

01-03 U.-J. Görke, A. Bucher, R. Kreißig. Ein Beitrag zur Materialparameteridentifikation bei finiten elastisch-plastischen Verzerrungen durch Analyse inhomogener Verschiebungsfelder mit Hilfe der FEM. Februar 2001.

01-04 R. A. Römer. Percolation, Renormalization and the Quantum-Hall Transition. February 2001.

01-05 A. Eilmes, R. A. Römer, C. Schuster, M. Schreiber. Two and more interacting particles at a metal-insulator transition. February 2001.

01-06 D. Michael. Kontinuumstheoretische Grundlagen und algorithmische Behandlung von ausgewählten Problemen der assoziierten Fließtheorie. März 2001.

01-07 S. Beuchler. A preconditioner for solving the inner problem of the p-version of the FEM, Part II - algebraic multi-grid proof. March 2001.

01-08 S. Beuchler, A. Meyer. SPC-PM3AdH v 1.0 - Programmer's Manual. March 2001.

01-09 D. Michael, M. Springmann. Zur numerischen Simulation des Versagens duktiler metallischer Werkstoffe (Algorithmische Behandlung und Vergleichsrechnungen). März 2001.

01-10 B. Heinrich, S. Nicaise. Nitsche mortar finite element method for transmission problems with singularities. March 2001.

01-11 T. Apel, S. Grosman, P. K. Jimack, A. Meyer. A New Methodology for Anisotropic Mesh Refinement Based Upon Error Gradients. March 2001.

01-12 F. Seifert, W. Rehm. (Eds.) Selected Aspects of Cluster Computing. March 2001.

01-13 A. Meyer, T. Steidten. Improvements and Experiments on the Bramble–Pasciak Type CG for mixed Problems in Elasticity. April 2001.

01-14 K. Ragab, W. Rehm. CHEMPI: Efficient MPI for VIA/SCI. April 2001.

01-15 D. Balkanski, F. Seifert, W. Rehm. Proposing a System Software for an SCI-based VIA Hardware. April 2001.

01-16 S. Beuchler. The MTS-BPX-preconditioner for the p-version of the FEM. May 2001.

01-17 S. Beuchler. Preconditioning for the p-version of the FEM by bilinear elements. May 2001.

01-18 A. Meyer. Programmer's Manual for Adaptive Finite Element Code SPC-PM 2Ad. May 2001.

01-19 P. Cain, M.L. Ndawana, R.A. Römer, M. Schreiber. The critical exponent of the localization length at the Anderson transition in 3D disordered systems is larger than 1. June 2001

01-20 G. Kunert, S. Nicaise. Zienkiewicz-Zhu error estimators on anisotropic tetrahedral and triangular finite element meshes. July 2001.

01-21 G. Kunert. A posteriori H^1 error estimation for a singularly perturbed reaction diffusion problem on anisotropic meshes. August 2001.

01-22 A. Eilmes, Rudolf A. Römer, M. Schreiber. Localization properties of two interacting particles in a quasi-periodic potential with a metal-insulator transition. September 2001.

01-23 M. Randrianarivony. Strengthened Cauchy inequality in anisotropic meshes and application to an a-posteriori error estimator for the Stokes problem. September 2001.

01-24 Th. Apel, H. M. Randrianarivony. Stability of discretizations of the Stokes problem on anisotropic meshes. September 2001.

The complete list of current and former preprints is available via
`http://www.tu-chemnitz.de/sfb393/preprints.html`.